7-27-2015

A Quantitative Perspective on Surface Marker Selection for the Isolation of Functional Tumor Cells

Calvin F. Cahall
University of Kentucky, calvin.cahall@uky.edu

Jacob L. Lilly
University of Kentucky, jacob.lilly@uky.edu

Edward A. Hirschowitz
University of Kentucky, edward.hirschowitz@uky.edu

Brad J. Berron
University of Kentucky, brad.berron@uky.edu

Right click to open a feedback form in a new tab to let us know how this document benefits you.

Follow this and additional works at: https://uknowledge.uky.edu/cme_facpub

Part of the Chemical Engineering Commons, and the Materials Science and Engineering Commons

A Quantitative Perspective on Surface Marker Selection for the Isolation of Functional Tumor Cells

A Quantitative Perspective on Surface Marker Selection for the Isolation of Functional Tumor Cells

Supplementary Issue: Breast Cancer Detection and Screening

Calvin F. Cahall[1,*], Jacob L. Lilly[1,*], Edward A. Hirschowitz[2] and Brad J. Berron[1]

[1]Department of Chemical and Materials Engineering, University of Kentucky, Lexington, KY, USA. [2]Division of Pulmonary and Critical Care Medicine, Department of Internal Medicine, University of Kentucky Chandler Medical Center, Lexington, KY, USA. *These authors contributed equally to this work.

ABSTRACT: Much effort has gone into developing fluid biopsies of patient peripheral blood for the monitoring of metastatic cancers. One common approach is to isolate and analyze tumor cells in the peripheral blood. Widespread clinical implementation of this approach has been hindered by the current choice of targeting epithelial markers known to be highly variable in primary tumor sites. Here, we review current antigen-based tumor cell isolation strategies and offer biological context for commonly studied cancer surface markers. Expression levels of the most common markers are quantitated for three breast cancer and two non-small cell lung cancer (NSCLC) lineage models. These levels are contrasted with that present on healthy peripheral blood mononuclear cells (PBMC) for comparison to expected background levels in a fluid biopsy setting. A key feature of this work is establishing a metric of markers per square micrometer. This describes an average marker density on the cell membrane surface, which is a critical metric for emerging isolation strategies. These results serve to extend expression of key tumor markers in a sensitive and dynamic manner beyond traditional positive/negative immunohistochemical staining to guide future fluid biopsy targeting strategies.

KEYWORDS: fluid biopsy, cell sorting, immunostaining, breast cancer, cancer lines

Introduction

From the first observation of tumor cells in the peripheral blood of cancer patients in 1869,[1] researchers have sought to establish the clinical relevance of finding these abnormal cells in circulation. Efforts have aimed toward developing a *fluid biopsy* in which patient-derived peripheral blood could be analyzed for circulating tumor cells (CTCs) with the goal of providing diagnostic and prognostic information with a minimally invasive procedure. While a correlative link between the presence of tumor cells in circulation and metastatic progression has been shown,[2–5] the current clinical utility of fluid biopsies remains questionable because of a lack of reliability and versatility to detect heterogeneous cancer cell types.[6,7]

Recent evidence suggests that multiple, distinct populations can arise from a single primary tumor with drastically variable phenotypic profiles.[8–10] While the exact mechanisms that generate and sustain these populations remain an area of intense research, it has been proposed that metastatic cells can be generally categorized as either: 1) primary epithelial tumor cells spilling into circulation through leaky vasculature or 2) primary tumor cells that have lost their epithelial nature and have actively migrated into the peripheral blood in a mesenchymal state. Once in systemic circulation, little is known about the biological functionality and fate that leads to colonization of metastatic foci at distant sites. Practically, functional characterization of CTCs has been encumbered by the extreme rarity at which they are seen of ~1/million. Further, many CTC isolation methods currently available require fixation and intracellular staining to determine epithelial identity, which prevents further examination of behavior and functionality after sorting. In order to fully bridge our understanding of the mechanisms that allow an epithelial cancer cell to survive in circulation and eventually spread the disease, viability of these rare cell populations must be preserved during enrichment. Thus, isolation must be based exclusively on unique surface receptors on the cell membrane that do not disrupt or compromise the integrity of the cell membrane.

In this study, we seek to quantify the surface expression level of these critical markers on common cell lines. This work represents a critical step in assessing the opportunities and limitations of isolating functional tumor-associated cells from peripheral blood. We have chosen tumor cell lines, as the majority of clinical research has centered on the utility of finding epithelial cells in circulation. Finally, we discuss the

significant limitations of using these in vitro cell models for CTCs in the study of rare cancer cell biology.

Current Technologies for Tumor Cell Isolation

Affinity-based separation is a microfluidic technique that achieves separation through the specific binding of cells to biomolecules immobilized within a microfluidic channel. Characteristic surface proteins have high affinity for the molecules, typically antibodies, that coat the channel walls and allow specific cell capture, while all other cells in the sample pass through without binding.[11] Nagrath et al develop this concept to separate viable CTCs from peripheral whole blood samples. CTCs are sorted using a microchip containing channel posts coated with antibodies against epithelial cell adhesion molecule (EpCAM).[12] Choi et al use microfluidic channels to allow cells to roll along the channel walls in an alternate direction of the bulk fluid flow. HL60 cells that express P-selectin glycoprotein ligand-1 bind to P-selectin-coated chips that allow specific capture, while preserving high viability compared to unsorted controls.[13] While this technique has shown promise for enrichment of viable cell populations, it has yet to be employed for epithelial CTC isolation.

Magnetic cell sorting or magnetically actuated cell sorting (MACS®, trademark of Miltenyi Biotec GmbH) is a sorting technique that relies on magnetic labeling of antigen positive populations. Magnetic beads are functionalized with specific antibodies that bind with surface proteins on the targeted cells. Once the targeted cells bind with the magnetic beads, the solution is placed in a magnetic field to separate the attached cells, and then the field is removed to collect the desired cells.[11] This method is capable of either batch or continuous flow processes and can separate up to 10^{11} cells in 30 minutes.[14] For samples with low concentrations of target cells, the purity of the isolated cells can be very low when compared to other separation techniques. Owen and Sykes show that for an initial target cell concentration of 1%, the enriched sample results in 37% purity of the target cell.[15] Owing to the low purities commonly achieved with magnetic sorting, this technique has commonly been used as a pre-enrichment step in conjunction with fluorescence activated cell sorting (FACS).

FACS is a microfluidic sorting method that was developed in the late 1960s and has become a standard clinical cell analysis tool. FACS involves fluorescently labeling specific proteins on cell surfaces, analyzing the cells individually, and then sorting into receptacles.[16,17] Modern machines are now capable of sorting based on 12 colors simultaneously along with two scattering parameters, forward scattering for size and fluorescent scattering.[16] Takao et al use FACS following magnetic pre-enrichment to isolate CTCs from whole blood. Enrichment was performed by positive selection using EpCAM microbeads and then analyzed using FACS where the mean detection efficiency was >95% with only a mean of 3% decrease in cell viability.[18] However, the ability of the cells to be separated depends on the ability to fluorescently tag the surface of the cell. The level of surface marker expression is ultimately a determining factor for sorting performance.

CellSearch® is the only FDA-approved method of CTC isolation for clinical prognosis that couples immunomagnetic enrichment with fluorescent staining of characteristic markers. CellSearch is specifically designed for the detection and enumeration of CTCs. The enrichment of these cells begins with magnetic sorting for EpCAM. The enriched population is then permeabilized and fluorescently labeled for cytokeratin and leukocyte common antigen (CD45) expressions to further confirm cell identity.[19] Clinical studies have shown statistical significance with prognosis and the number of CTCs detected for breast, prostate, and colorectal cancers.[2,4,20] The cutoff concentration for determining poorer prognosis in metastatic breast cancer and metastatic prostate cancer is ≥5 CTCs/7.5 mL of peripheral blood and ≥3 CTCs/7.5 mL of peripheral blood in metastatic colorectal cancer. Enumeration of CTCs above the cutoff has shown a significantly lower progression-free survival time and overall survival time than patients with fewer CTCs than the cutoff.[19,20] While CellSearch is effective for the detection and enumeration of CTCs, it does not isolate viable cells. This limitation stems from the low purity after the immunomagnetic enrichment, requiring confirmation of CTC status by intracellular cytokeratin staining.

While antigen-based isolation methods have shown the greatest promise toward a clinically useful fluid biopsy, these strategies are critically dependent on the level of antigen expression presented on target cells. Low quantities, and more specifically low densities, of the target marker will decrease the net binding recognition of antibodies to a marker positive cell surface, potentially leading to poor discrimination between positive and negative events. Critically, the current literature poorly describes the expression of even the best-known tumor markers on the most commonly studied tumor cell lines. Typically, the expression of a marker is communicated as positive or negative. At best, papers will communicate relative levels in terms of dim, moderate, bright, or variable. Alternatively, the level of receptor expression is given as moles of receptor per mass of cell lysate. Techniques that have been used to detect cell antigens qualitatively and quantitatively include enzyme immunoassay (EIA) and enzyme-linked immunosorbent assay (ELISA).[21,22] However, these techniques that quantify expression on a total mass basis are minimally useful in the development of viable cell sorting, as they report antigens that may be present only intracellularly and unavailable for targeting on an intact, viable cell.[23,24]

Cancer-associated Surface Biomarkers

Since most primary tumors are epithelial in nature, epithelial markers are commonly targeted for isolation of tumor cells in peripheral blood. Of these, the EpCAM is by far the most prevalent in literature. EpCAM is a calcium ion-independent protein that is responsible for homophilic cell-to-cell adhesion,[25] and it has been shown to be overexpressed

in breast cancer specimens by 100–1000-fold relative to the normal tissue.[26] A critical limitation of isolation based on EpCAM is the prevalence of both EpCAM negative tumor sites and loss of epithelial markers on cancer cells during the transition to the more invasive, mesenchymal phenotype.

Particularly in breast cancer, molecular classification of cancer subtype is conventionally based on human epidermal growth factor receptor 2 (HER2), estrogen receptor (ER), and progesterone receptor (PR). These molecules are commonly targeted for breast cancer therapies, and their expression is used in both therapy selection and prognosis. HER2 is a tyrosine kinase that forms heterodimers with epidermal growth factor receptor (EGFR), HER3, or HER4 to promote cell division.[27,28] ER binds the hormone estrogen, where ligand binding stimulates the proliferation of mammary cells. Overexpression of ER is hypothesized to contribute to breast cancer progression through increased cell division and DNA production and/or formation of genotoxic by-products.[29] PR is a hormone receptor that is activated by the progesterone ligand and is a transcription protein for the regulation of specific genes.[30] Some studies suggest that expression of PR is controlled by expression of ER.[31]

CD44 expression has been widely shown to correlate with cancer metastasis. CD44 is a transmembrane adhesion receptor that primarily binds to the glycosaminoglycan hyaluronan in the extracellular matrix[32] and exhibits several different tissue-specific isoforms. Activation of CD44 by hyaluronan has been observed to stimulate intracellular signaling of cellular functions such as adhesion, migration, and invasion, which are key functions in cancer metastasis and progression.[33,34] A recent study showed elevated counts of CD44$^+$/CD24$^-$ CTCs in samples of metastatic breast cancer patients.[9]

E-Cadherin is a transmembrane, calcium-dependent, homotypic cell-to-cell adhesion protein. The decreased expression of this adhesion molecule is the first step in the progression of metastatic cancer by allowing the detachment of cells from the primary site[35] and is a hallmark of epithelial-to-mesenchymal transitions.[36] Like E-cadherin, N-cadherin is a calcium-dependent, homotypic cell-to-cell adhesion molecule. However, N-cadherin expression is indicative of invasive and metastatic breast cancers.[37,38] While N-cadherin is an adhesion molecule, it is believed to be responsible for the attachment as well as the detachment of cancer cells from the primary tumor and to the distant tissue.[37] The increased expression of N-cadherin is often coupled with the decrease of E-cadherin in the transition of the epithelial-to-mesenchymal phenotype, which is commonly referred to as *cadherin switch*.[38]

Integrins are a family of cell surface adhesion proteins involved in the attachment of cells to the extracellular matrix and play key roles in migration, survival, and activation of apoptosis suppresors.[39] In particular, integrin αVβ3 has been identified as a key player in tumor growth, invasion, early angiogenic activity, and metastasis.[40] αVβ3 binds several ligands from the extracellular matrix, positively regulates cell migration, and is

overexpressed in breast cancer metastatic lesions.[41] ICAM-1 is another cancer-associated[42,43] surface adhesion molecule that plays a role in morphology, cell-to-cell interactions, and cell migration.[44] These roles of ICAM-1 along with its positive expression found in CTCs suggest that this protein is intimately involved in metastasis by controlling the movement of cells through the extracellular matrix.[44] In addition to invasive potential, the proliferation and angiogenic potential of tumor cells are critical to disease progression. EGFR is a transmembrane protein that belongs to the same family of tyrosine kinases as HER2. EGFR is a ligand activated by both epidermal growth factor (EGF), and transforming growth factor-alpha (TGF-α), which ultimately controls processes such as proliferation, angiogenesis, and inhibition of apoptosis.[45] Positive expression of EGFR in breast carcinomas has been linked to poorer prognosis over EGFR-negative tumors.[46]

Methods

Cell culture. Three breast cancer cell lines and two non-small cell lung cancer (NSCLC) cell lines were cultured. Breast cancer lines included MDA-MB-231 (mammary adenocarcinoma), MCF-7 (mammary adenocarcinoma), and T-47D (mammary ductal carcinoma), and NSCLC lines included A549 (alveolar adenocarcinoma) and H358 (bronchioalveolar carcinoma). All tumor lines were cultured in RPMI-1640 growth medium (HyClone) supplemented with 2.05 mM L-glutamine, 10% fetal bovine serum (FBS; Fisherbrand), and 1% penicillin-streptomycin (Sigma-Aldrich) and maintained at 5% CO_2 in air and 37°C. Cells were cultured for 48 hours and were approximately 60–80% confluent just before experimentation. Additionally, a peripheral blood control sample was graciously provided by Dr. Hainsworth Shin and processed within an hour of collection. Briefly, whole blood was mixed with a dextran/NaCl solution to a working concentration of 2 wt% dextran and 0.3 wt% NaCl and was allowed to separate by $1 \times g$ sedimentation at room temperature for one hour. The buffy coat containing peripheral blood mononuclear cells (PBMC) was then pipetted off and exposed to red blood cell lysis buffer (155 mM NH_4Cl, 10 mM $KHCO_3$, 0.1 mM EDTA) for five minutes to further remove red blood cells from the sample. The nucleated cells were collected by centrifugation at $300 \times g$ for five minutes and washed twice with cold $1 \times$ phosphate-buffered saline (PBS).

Cell imaging. Representative bright field, phase-contrast images of all tumor cell lines were taken with a Nikon Ti-U inverted microscope.

Surface marker immunostaining. Tumor cells were incubated with trypsin/EDTA (0.25%) solution for three minutes to allow for detachment, rinsed with growth medium, and centrifuged. Cell concentration and cell diameter were determined optically with a Cellometer automated cell counter (Nexcelom). Each data replicate sample consisted of 1×10^5 cells in a microcentrifuge tube. For experimentation, a rinsing buffer of $1 \times$ PBS with 3% FBS was prepared and used for all

rinsing steps. All materials and cell samples were kept on ice throughout the staining procedure. For immunolabeling, cell samples were first rinsed once with rinsing buffer and centrifuged ($400 \times g$, 1.5 minutes). Subsequently, samples were incubated with primary antibodies at ~0.5 μg in 150 μL of rinsing buffer for 40 minutes. For all cell lines, markers were targeted with primary monoclonal mouse IgG antibodies with the corresponding isotype controls that consisted of CD326/EpCAM (IgG2b, clone 9C4, BioLegend), HER1/EGFR (IgG1, clone AY13, BioLegend), CD44 (IgG1, clone BJ18, BioLegend), E-cadherin (IgG1, clone 67A4, BioLegend), erbB2/HER2 (IgG1, clone 24D2, BioLegend), N-cadherin (IgG1, clone8C11, BioLegend), αVβ3 integrin (IgG1, clone 23C6, BioLegend), ICAM-1 (IgG1, clone HA58, eBioscience, San Diego, CA), and ER-α (IgG2a, clone F-10, Santa Cruz Biotechnology). Samples were then rinsed twice with rinsing buffer on ice, with centrifugation between rinses. Cells were then labeled with biotinylated goat anti-mouse IgG antibody (Vector Labs) at a 1:400 dilution in rinsing buffer on ice for 40 minutes. Cells were rinsed twice with rinsing buffer and incubated with streptavidin (SA)-phycoerythrin (PE) at ~1 μg in 200 μL on ice for 20 minutes. Samples were rinsed three times and resuspended in ~200 μL rinsing buffer for immediate analysis.

Flow cytometry. Cell sample immunofluorescence was assessed with an Accuri C6 flow cytometer. Samples were kept on ice and then gently vortexed before a cytometry run. For each replicate, 5000 cell events were collected based on initial cell culture control gating. PE fluorescence data were collected for each sample in the FL2 channel configured for excitation with a 488-nm laser, and emission was detected through a 585/40 bandpass filter.

Data analysis. Data are calculated as mean ± standard error of the mean (s.e.m.) ($N = 3$) for all marker quantification assays and cell diameter calculations. Standard deviation within individual replicates is also reported in Supplementary Figure 3. The calibration of QuantiBRITE PE bead was performed every day of cell immunofluorescence data collection, and fluorescence calibration values were collected in channel FL2. PE per cell values were calculated using a linear calibration curve ($R^2 = \sim 0.98$) of number of PE molecules vs. FL2 fluorescence generated from the bead calibration of each on their respective days of collection (Supplementary Fig. 1). Statistical analysis consisted of a two-tailed student's t-test performed in Matlab to calculate P-values (Supplementary Table 1).

Results

Imaging analysis. A summary of cell types and the corresponding cell sizes is shown in Table 1. From a regression analysis relating mean forward scatter and mean Cellometer cell size, cell diameters of individual populations of lymphocytes, monocytes, and granulocytes were extrapolated. As expected, these PBMC showed diameters smaller than epithelial cancer cells. To estimate cell surface area, a spherical model was assumed for each cell. While some cell types can possess membrane folds that can alter diameter and surface area in certain scenarios[47] (e.g. activation of white blood cells), we posit this simple model is sufficient to generally show accessible marker densities on the surface of the cells studied here. For morphological comparison, representative bright field images of tumor cell lines are shown in Figure 1. The basal-like breast line MDA-MB-231[48] shows morphology quite distinct from any other investigated in the study, with elongated, multi-polar behavior and favoring minimal cell–cell contact consistent with basal subtypes. Luminal breast lines MCF-7 and T-47D[49] and NSCLC line H358 show morphology more consistent with an epithelial phenotype favoring extensive cell–cell contact and colonization. NSCLC line A549 appears to exhibit behavior somewhere between these extremes with less organized cell junctions.

Quantitation of marker expression by flow cytometry. The results of marker quantitation using the flow cytometric QuantiBRITE bead assay are presented in Figures 2 and 3, where PE fluorescence serves as a reporter for antigen quantity. Expression data are presented here as expression fold over isotype controls as well as normalized to the calculated mean surface area for each cell type. Because we employed an indirect immunostaining approach, some labeling amplification inherent in antibody binding interactions was seen.

Table 1. Summary of cell types analyzed in the study. Diameter and surface area calculations are reported as mean ± s.e.m.

| CELL TYPE	DESCRIPTION	DIAMETER (μm)	SURFACE AREA (μm²)
MDA-MB-231	Mammary adenocarcinoma	11.5 ± 0.3	415 ± 19
MCF-7	Mammary adenocarcinoma	17.1 ± 0.4	922 ± 43
T-47D	Mammary ductal carcinoma	14.5 ± 0.3	663 ± 34
A549	Alveolar adenocarcinoma	15.0 ± 0.4	710 ± 38
H358	Bronchioalveolar carcinoma	16.8 ± 0.5	890 ± 47
Peripheral lymphocytes	Healthy PBMC	6.7 ± 0.1	142 ± 1
Peripheral monocytes	Healthy PBMC	7.9 ± 0.1	197 ± 2
Peripheral granulocytes	Healthy PBMC	8.2 ± 0.1	209 ± 1
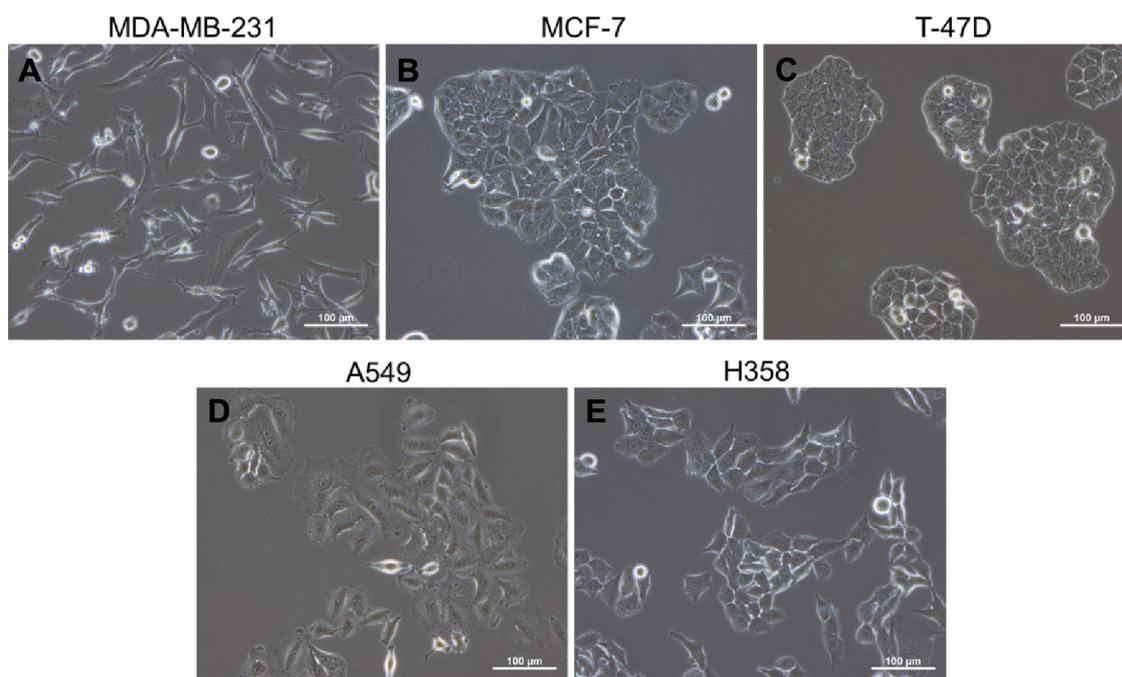
Figure 1. Representative bright field micrograph images of cultured breast cancer lines (MDA-MB-231, MCF-7, T-47D) and NSCLC lines (A549, H358).

In Supplementary Figure 2, a biotin anti-EpCAM primary was labeled in parallel to biotin-anti-mouse secondary staining, with a 1.3-fold amplification seen for secondary immunolabeling. Further, we also expect some amplification at the biotin/SA-PE labeling interaction. Although this may skew the representation of the actual number of biological copies of these surface proteins, the focus of our study was to provide a methodology engineering perspective on the maximum level of antigen affinity recognition afforded by traditional immunolabeling for viable CTC isolation, where some amplification is not only acceptable but desired. Moreover, as all markers were tagged with identical indirect staining approaches, relative expression across cell lines and between markers should be consistent regardless of any labeling amplification.

Overall, marker expression levels often varied drastically between cell lines with some correlation seen between cell morphology, behavior, and marker profiles. Specifically, MDA-MB-231 showed significantly decreased PE labeling density for EpCAM and E-cadherin compared to MCF-7, T-47D, and H358 (P-values $<$ 0.001), while showing higher levels of labeling density for CD44, EGFR, and ICAM-1 (P-values $\leq$ 0.01, Fig. 3). A549 also showed decreased EpCAM and E-cadherin density (P-values $<$ 0.001) and increased CD44 density over MCF-7, T-47D, and H358 (P-values $<$ 0.01). EGFR and ICAM-1 expression seemed to be consistently high, resulting in PE label densities equal to or greater than $100/\mu m^2$ for all cell lines except MCF-7. EGFR has been linked to a basal-like molecular signature,[50] and elevated levels of EGFR and ICAM-1 have been linked to metastatic disease.[44,51] The αV-$\beta 3$ integrin is elevated 10-fold in MDA-MB-231 cells compared to the other tumor lines

investigated (P-values $<$ 0.001), with ~30 PE molecules per square micrometer. Of particular interest for breast cancer lines was ERα and HER2 expression because of their prominent clinical role in breast cancer classification, prognosis, and therapy selection. The antibody chosen (clone F-10, Santa Cruz Biotechnology) targeted the c-terminus ligand binding domain. All three breast cancer lines showed a slight increase in ERα expression over isotype controls (P-values $<$ 0.05, Fig. 2A–C) and a statistical elevation in expression over NSCLC lines (P-values $<$ 0.05), which showed virtually no ERα expression, with the exception of MCF-7 compared to A549 (P = 0.15, Fig. 2D and E). HER2 expression was expressed at relatively high levels in all three breast cancer lines as well as NSCLC lines, resulting in roughly 50–100 PE molecules per square micrometer (Fig. 3).

Our study also sought to provide background expression levels on PBMC for comparison, as it is ultimately a determining factor in marker selection for isolating CTCs from peripheral blood. Figure 2F shows marker expression fold over IgG for separately gated lymphocyte, monocyte, and granulocyte populations. Notably, relatively elevated levels of both CD44 and ICAM-1 are seen. In Figure 3F, the PE binding density is reported for PBMC, showing high non-specific noise in isotype controls, especially for monocytes. This immunolabeling noise can reduce the biorecognition contrast between the target tumor cells for capture and the majority PBMC; hence, here we further demonstrate the PE labeling density fold vs. peripheral blood monocyte expression, which represents the most likely culprits for false-positive capture (Fig. 4). First, MDA-MB-231 showed drastically attenuated EpCAM (P = 0.0038) and E-cadherin
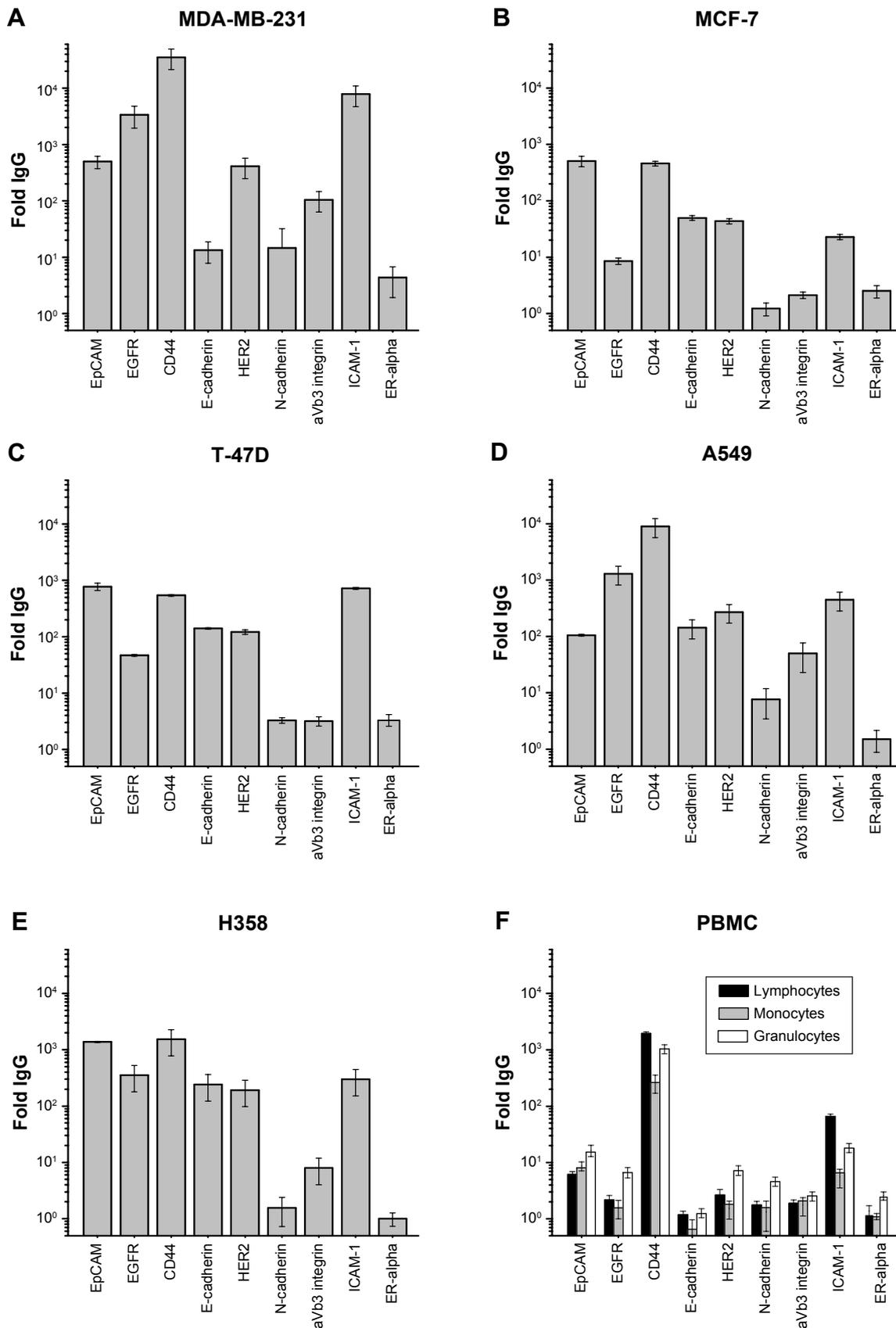
Figure 2. Summary of tumor marker expression on viable cells. Presented as fold over isotype controls for cancer lines and healthy PBMC as quantified by flow cytometry analysis of a PE reporter label. All data are reported as mean ± s.e.m.
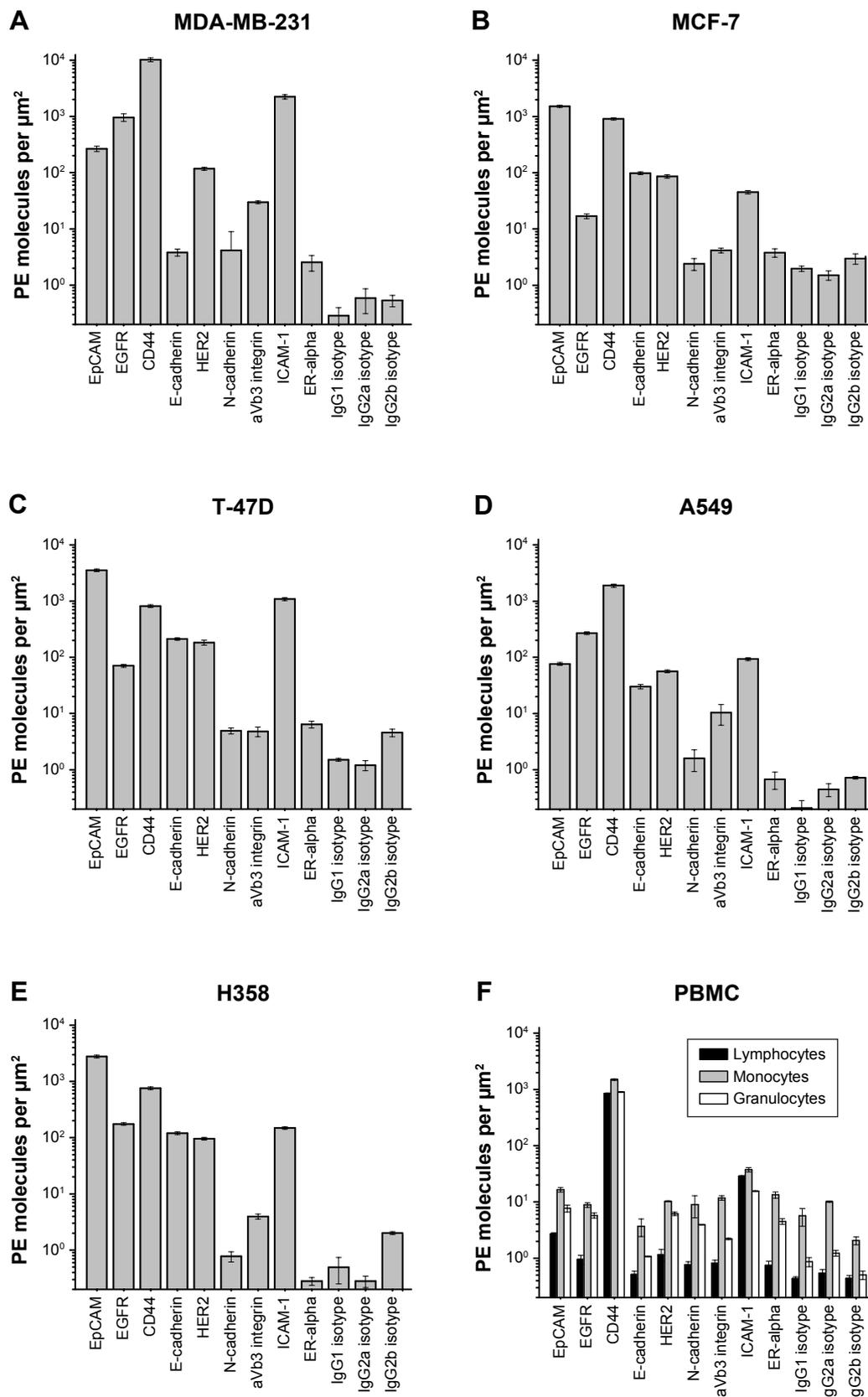
Figure 3. Summary of PE labeling density (number of PE molecules per square micrometer of cell surface) for various tumor marker targeting conditions on viable cancer line cells and healthy PBMC. All data are reported as mean ± s.e.m. The corresponding antibody isotypes are as follows—IgG1: EGFR, CD44, E-cadherin, HER2, N-cadherin, aVb3 integrin, ICAM-1; IgG2a: ER-alpha; and IgG2b: EpCAM.

Figure 4. Summary of PE labeling density of all cancer lines studied presented as fold expression over healthy monocytes from a peripheral blood sample. Data are reported as mean ± s.e.m.

($P = 0.90$) elevation over monocytes because of low expression seen in Figure 3A. EGFR contrast remains high for MDA-MB-231 and NSCLC lines (P-values $<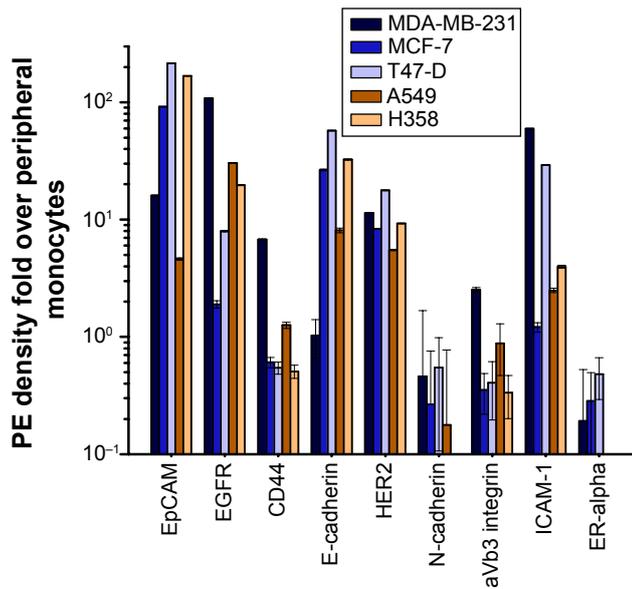 0.01$). Although CD44 and ICAM-1 were highly expressed across all cancer lines in the study, the contrast over blood cells is reduced because of the corresponding high expression in PBMC. MDA-MB-231 has a slight CD44 contrast over monocytes, and MDA-MB-231 and A549 both retain high contrast for ICAM-1 expression (P-values < 0.01). Finally, N-cadherin and αV-β3 integrin expression on all five cancer lines investigated shows little-to-no elevation over that of peripheral monocytes.

Discussion

Here, we have reported quantitative results of levels of antibody-mediated recognition attained for several commonly investigated markers associated with metastasis on both breast cancer and NSCLC lines. To our knowledge, very little information is reported on the numbers of marker proteins present on cancer cell membrane surfaces. While many fundamental biology questions can be answered with immunohistochemical and blotting assays that yield binned positive/negative information, these approaches generally fail to represent the highly dynamic and variable expression patterns seen for many tumor cells.[24,52,53] Particularly for antibody-based cell isolation methodologies, the ability to capture a marker-presenting cell among a majority of marker-negative cells is critically dependent on the amount of marker proteins available on the cell surface for labeling. In this light, we propose that these findings represent a significant step toward providing the tumor cell isolation community with quantitative antigenic expression information.

Notably, our results show distinct expression signatures for basal and luminal breast cancer subtypes consistent with the characteristics commonly associated with each. Basal-like cells are often seen to be more highly invasive and dedifferentiated, while luminal-type cells are often considered epithelial like.[49,50] MDA-MB-231 are classified as basal, whereas MCF-7 and T-47D are luminal A subtypes. We found that MDA-MB-231 showed elevated levels of mesenchymal and/or metastatic markers CD44, N-cadherin, αV-β3 integrin, and ICAM-1 as well as upregulation of EGFR (commonly seen for basal subtypes) (Fig. 2A).[50] Further, the basal-like MDA-MB-231 also showed lower expression of epithelial markers EpCAM and E-cadherin compared to MCF-7 and T-47D (Fig. 2A–C). Elevated levels of mesenchymal markers have been linked to a more metastatic phenotype, as these proteins play key functional roles as tools for migration and invasion.[54] In the context of CTC isolation that currently is predominantly based on EpCAM+ sorting, these results highlight a disconnection between marker targeting strategy and the biological tendencies of highly invasive cells. Specifically, a detection threshold of EpCAM expression exists for any antibody-based isolation methodology, and highly invasive cells downregulate EpCAM and have a higher potential to go unseen as false negatives.

A surprising result was also seen for ERα expression in comparing the basal (MDA-MB-231) and luminal A (MCF-7 and T-47D) subtypes in the study. All three cell lines showed a similar expression of HER2, which was not unexpected for basal and luminal A subtypes that generally do not have overexpression of HER2.[49] However, we found that MDA-MB-231 cells also expressed similar surface densities of ERα compared to MCF-7 and T-47D. One possible explanation could be that because our focus was to determine antigen densities on intact tumor cell surfaces, the antibody chosen for ERα targeting (clone F-10, Santa Cruz Biotech) targeted the C-terminal ligand binding domain; however, these nuclear receptors are often trafficked intracellularly.[55] Therefore, these results do not account for intracellular ERα where differences in expression between basal and luminal A subtypes could arise.

Our study also sought to offer some order-of-magnitude perspective on expression levels of surface markers CD44, N-cadherin, αV-β3 integrin, and ICAM-1 implicated in metastatic progression,[39,44,56] as these could potentially serve as promising new targets for sorting clinically relevant cells. A poorly expressed molecule may play an important role biologically, but would be of minimal utility as a target for live cell isolation. Furthermore, a molecule may even be highly expressed, but if it is also highly expressed on peripheral blood cells, it would no longer serve to distinguish epithelial identity from the background blood cells. PBMC marker expression was normalized to cell size similar to epithelial cells, and PBMC size estimates were found to be in fair agreement with literature.[57,58] We found that although both N-cadherin and αV-β3

integrin were upregulated on some lines (MDA-MB-231 and A549), their inherent expression density was still approximately equal to or below the expression found on peripheral monocytes, which consistently showed the highest background staining levels (Figs. 3F and 4). Additionally, while CD44 was relatively high for all cancer lines (Fig. 3), it was also highly expressed in PBMC, which reduced the expression ratio over monocytes to nearly 1 or below for all lines except MDA-MB-231 that retained a seven-fold ratio over monocytes (Fig. 4). Therefore, because our results show minimal differences in expression of these markers over blood cells, they are not recommended for targeting intact tumor cells. It is worth noting though that more work is warranted in quantitating the extent of elevation of markers like N-cadherin, which are shown to undergo a cadherin switch from stromal cytokine stimulation in vivo.[59,60] This phenotypic transition is correlated with a more invasive cell and could conceivably potentiate N-cadherin as a target for tumor cell isolation. ICAM-1 expression density was seen to be approximately 30-to-60-fold higher than monocytes for T-47D and MDA-MB-231, respectively (Fig. 4). ICAM-1 is involved in cell adhesion interactions and migration and has been recently been classified as a mesenchymal cell marker.[61–63] Further, one recent study has shown that increased populations of ICAM-1^{high} CTCs correlated to poorer prognosis in hepatocellular carcinoma patients.[44] Coupled with these findings, our results point toward ICAM-1 as a potential target for isolation of clinically relevant tumor cells.

In conclusion, we have reported surface marker densities on several model tumor cell lineages to guide the development of isolation methodologies for live and functional CTC populations. The surface density of targeted markers is a critical parameter for any antigen-based CTC capture platform and likely represents a key oversight that has led to poor performance of many previously developed technologies. Our results also indicate extreme variability in expression between markers and cancer cell lines and illustrate the need for greater appreciation of heterogeneity at the surface marker level across different cancer subsets. While the values in Figures 2 and 3 are presented as mean ± s.e.m, Supplementary Figure 3 also shows that the variance in immunofluorescence for cell events within each replicate was often considerably higher. This could be due in part to the inherent variability within the cultured cell population as well as deviations from the mean K_d for each antibody used. As with any antibody-based assay, the variance in antibody binding affinity from different suppliers should be carefully considered when interpreting these data as well as in designing an antibody-based isolation strategy. Further, cancer heterogeneity has also been widely reported for in vivo settings.[53,64] Cytokine signaling and tumor–stromal interactions can cause certain subsets of malignant cells to display drastically altered marker profiles, some resembling stem-like phenotypes in what is referred to as epithelial–mesenchymal transition.[8] These highly potent subsets have been reported to go largely unnoticed in EpCAM based isolation strategies, leading many to suggest that perhaps EpCAM alone is not sufficient to capture any and all CTCs.[6,65] Our findings further support that EpCAM surface presentation cannot be assumed to be similar for all tumor lines, and more comprehensive targeting strategies that account for expression-level variability is warranted. One possible strategy would be to use panels of antibodies to target several tumor markers to ensure successful capture in instances where certain markers are downregulated. For example, Yu et al targeted patient-derived breast CTCs with a cocktail of EpCAM, EGFR, and HER2 antibodies in a microchip device approach, where subsequent fluorescent immunostaining of captured cells revealed that they possessed highly variable and dynamic phenotypes with both epithelial and mesenchymal markers.[52] Building upon these types of robust targeting strategies will be vital for developing future generations of more clinically relevant fluid biopsy technologies.

Author Contributions
Conceived and designed the experiments: BJB and JLL. Analyzed the data: CFC and JLL. Wrote the first draft of the manuscript: CFC and JLL. Contributed to the writing of the manuscript: EAH and BJB. Agree with manuscript results and conclusions: CFC, JLL, EAH, and BJB. Jointly developed the structure and arguments for the paper: BJB and JLL. Made critical revisions and approved final version: EAH and BJB. All authors reviewed and approved of the final manuscript.

Supplementary Materials
Supplementary table 1. Summary of student's *t*-test calculations for surface marker data.

Supplementary figure 1. Plot of regression analysis relating mean forward scatter vs. mean Cellometer cell diameter for all five cancer lines.

Supplementary figure 2. PE labeling per cell comparison for indirect staining conditions on viable A549 cells. Labeling conditions before SA-PE incubation were (left) covalently biotinylated mouse anti-human EpCAM and (right) mouse anti-human EpCAM + biotinylated goat anti-mouse. Data are reported as mean ± s.e.m.

Supplementary figure 3. Summary of PE labeling per cell for all markers and cell types. Error bars represent the standard error of events collected by flow cytometry. The corresponding antibody isotypes are as follows—IgG1: EGFR, CD44, E-cadherin, HER2, N-cadherin, aVb3 integrin, ICAM-1; IgG2a: ER-alpha; and IgG2b: EpCAM.

REFERENCES

1. Ashworth T. A case of cancer in which cells similar to those in the tumours were seen in the blood after death. *Aust Med J*. 1869;14(3):146–149.

2. Cohen SJ, Punt CJ, Iannotti N, et al. Relationship of circulating tumor cells to tumor response, progression-free survival, and overall survival in patients with metastatic colorectal cancer. *J Clin Oncol*. 2008;26(19):3213–3221.

3. Cristofanilli M, Budd GT, Ellis MJ, et al. Circulating tumor cells, disease progression, and survival in metastatic breast cancer. *N Engl J Med*. 2004;351(8):781–791.

4. de Bono JS, Scher HI, Montgomery RB, et al. Circulating tumor cells predict survival benefit from treatment in metastatic castration-resistant prostate cancer. *Clin Cancer Res*. 2008;14(19):6302–6309.

5. Miller MC, Doyle GV, Terstappen LW. Significance of circulating tumor cells detected by the CellSearch system in patients with metastatic breast colorectal and prostate cancer. *J Oncol*. 2010;2010:617421.

6. Gorges TM, Tinhofer I, Drosch M, et al. Circulating tumour cells escape from EpCAM-based detection due to epithelial-to-mesenchymal transition. *BMC Cancer*. 2012;12(1):178.

7. Wicha MS, Hayes DF. Circulating tumor cells: not all detected cells are bad and not all bad cells are detected. *J Clin Oncol*. 2011;29(12):1508–1511.

8. Kalluri R, Weinberg RA. The basics of epithelial–mesenchymal transition (vol 119, pg 1420, 2009). *J Clin Invest*. 2010;120(5):1786–1786.

9. Aktas B, Tewes M, Fehm T, Hauch S, Kimmig R, Kasimir-Bauer S. Stem cell and epithelial-mesenchymal transition markers are frequently overexpressed in circulating tumor cells of metastatic breast cancer patients. *Breast Cancer Res*. 2009;11(4):R46.

10. Bonnomet A, Brysse A, Tachsidis A, et al. Epithelial-to-mesenchymal transitions and circulating tumor cells. *J Mammary Gland Biol Neoplasia*. 2010;15(2):261–273.

11. Bhagat AAS, Bow H, Hou HW, Tan SJ, Han J, Lim CT. Microfluidics for cell separation. *Med Biol Eng Comput*. 2010;48(10):999–1014.

12. Nagrath S, Sequist LV, Maheswaran S, et al. Isolation of rare circulating tumour cells in cancer patients by microchip technology. *Nature*. 2007;450(7173):1235–1239.

13. Choi S, Karp JM, Karnik R. Cell sorting by deterministic cell rolling. *Lab Chip*. 2012;12(8):1427–1430.

14. Thiel A, Scheffold A, Radbruch A. Immunomagnetic cell sorting—pushing the limits. *Immunotechnology*. 1998;4(2):89–96.

15. Owen CS, Sykes NL. Magnetic labeling and cell sorting. *J Immunol Methods*. 1984;73(1):41–48.

16. Herzenberg LA, Parks D, Sahaf B, Perez O, Roederer M, Herzenberg LA. The history and future of the fluorescence activated cell sorter and flow cytometry: a view from Stanford. *Clin Chem*. 2002;48(10):1819–1827.

17. Ibrahim SF, van den Engh G. High-speed cell sorting: fundamentals and recent advances. *Curr Opin Biotechnol*. 2003;14(1):5–12.

18. Takao M, Takeda K. Enumeration, characterization, and collection of intact circulating tumor cells by cross contamination-free flow cytometry. *Cytometry A*. 2011;79(2):107–117.

19. Allard WJ, Matera J, Miller MC, et al. Tumor cells circulate in the peripheral blood of all major carcinomas but not in healthy subjects or patients with nonmalignant diseases. *Clin Cancer Res*. 2004;10(20):6897–6904.

20. Cristofanilli M, Hayes DF, Budd GT, et al. Circulating tumor cells: a novel prognostic factor for newly diagnosed metastatic breast cancer. *J Clin Oncol*. 2005;23(7):1420–1430.

21. Gan SD, Patel KR. Enzyme immunoassay and enzyme-linked immunosorbent assay. *J Invest Dermatol*. 2013;133(9):e12.

22. Paulie S, Perlmann H, Perlmann P. Enzyme-linked Immunosorbent Assay. *eLS*. 2003;1–4.

23. Konecny G, Pauletti G, Pegram M, et al. Quantitative association between HER-2/neu and steroid hormone receptors in hormone receptor-positive primary breast cancer. *J Natl Cancer Inst*. 2003;95(2):142–153.

24. McCabe A, Dolled-Filhart M, Camp RL, Rimm DL. Automated quantitative analysis (AQUA) of in situ protein expression, antibody concentration, and prognosis. *J Natl Cancer Inst*. 2005;97(24):1808–1815.

25. Königsberg R, Obermayr E, Bises G, et al. Detection of EpCAM positive and negative circulating tumor cells in metastatic breast cancer patients. *Acta Oncol*. 2011;50(5):700–710.

26. Osta WA, Chen Y, Mikhitarian K, et al. EpCAM is overexpressed in breast cancer and is a potential target for breast cancer gene therapy. *Cancer Res*. 2004;64(16):5818–5824.

27. Jain J, Veggiani G, Howarth M. Cholesterol loading and ultrastable protein interactions determine the level of tumor marker required for optimal isolation of cancer cells. *Cancer Res*. 2013;73(7):2310–2321.

28. Eccles SA. The role of c-erbB-2/HER2/neu in breast cancer progression and metastasis. *J Mammary Gland Biol Neoplasia*. 2001;6(4):393–406.

29. Deroo BJ, Korach KS. Estrogen receptors and human disease. *J Clin Invest*. 2006;116(3):561.

30. Osborne CK, Yochmowitz MG, Knight WA, McGuire WL. The value of estrogen and progesterone receptors in the treatment of breast cancer. *Cancer*. 1980;46(S12):2884–2888.

31. McGuire W, Horwitz K, Pearson O, Segaloff A. Current status of estrogen and progesterone receptors in breast cancer. *Cancer*. 1977;39(6):2934–2947.

32. Lopez JI, Camenisch TD, Stevens MV, Sands BJ, McDonald J, Schroeder JA. CD44 attenuates metastatic invasion during breast cancer progression. *Cancer Res*. 2005;65(15):6755–6763.

33. Afify A, Purnell P, Nguyen L. Role of CD44s and CD44v6 on human breast cancer cell adhesion, migration, and invasion. *Exp Mol Pathol*. 2009;86(2):95–100.

34. Toole BP. Hyaluronan promotes the malignant phenotype. *Glycobiology*. 2002;12(3):37R-42R.

35. Perl A-K, Wilgenbus P, Dahl U, Semb H, Christofori G. A causal role for E-cadherin in the transition from adenoma to carcinoma. *Nature*. 1998;392(6672):190–193.

36. Hajra KM, Ji X, Fearon ER. Extinction of E-cadherin expression in breast cancer via a dominant repression pathway acting on proximal promoter elements. *Oncogene*. 1999;18(51):7274–7279.

37. Hazan RB, Phillips GR, Qiao RF, Norton L, Aaronson SA. Exogenous expression of N-cadherin in breast cancer cells induces cell migration, invasion, and metastasis. *J Cell Biol*. 2000;148(4):779–790.

38. Yilmaz M, Christofori G. EMT, the cytoskeleton, and cancer cell invasion. *Cancer Metastasis Rev*. 2009;28(1–2):15–33.

39. Jin H, Varner J. Integrins: roles in cancer development and as treatment targets. *Br J Cancer*. 2004;90(3):561–565.

40. Hood JD, Cheresh DA. Role of integrins in cell invasion and migration. *Nat Rev Cancer*. 2002;2(2):91–100.

41. Beer AJ, Niemeyer M, Carlsen J, et al. Patterns of αvβ3 expression in primary and metastatic human breast cancer as shown by 18F-Galacto-RGD PET. *J Nucl Med*. 2008;49(2):255–259.

42. O'hanlon D, Fitzsimons H, Lynch J, Tormey S, Malone C, Given H. Soluble adhesion molecules (E-selectin, ICAM-1 and VCAM-1) in breast carcinoma. *Eur J Cancer*. 2002;38(17):2252–2257.

43. Budinsky AC, Brodowicz T, Wiltschke C, et al. Decreased expression of ICAM-1 and its induction by tumor necrosis factor on breast-cancer cells in vitro. *Int J Cancer*. 1997;71(6):1086–1090.

44. Liu S, Li N, Yu X, et al. Expression of intercellular adhesion molecule 1 by hepatocellular carcinoma stem cells and circulating tumor cells. *Gastroenterology*. 2013;144(5):1031–1041.

45. Bhargava R, Gerald WL, Li AR, et al. EGFR gene amplification in breast cancer: correlation with epidermal growth factor receptor mRNA and protein expression and HER-2 status and absence of EGFR-activating mutations. *Mod Pathol*. 2005;18(8):1027–1033.

46. Harris AL, Nicholson S, Richard J, Sainsbury C, Farndon J, Wright C. Epidermal growth factor receptors in breast cancer: association with early relapse and death, poor response to hormones and interactions with neu. *J Steroid Biochem*. 1989;34(1):123–131.

47. Dewitt S, Hallett M. Leukocyte membrane "expansion": a central mechanism for leukocyte extravasation. *J Leukoc Biol*. 2007;81(5):1160–1164.

48. Chavez KJ, Garimella SV, Lipkowitz S. Triple negative breast cancer cell lines: one tool in the search for better treatment of triple negative breast cancer. *Breast Dis*. 2010;32(1):35–48.

49. Holliday DL, Speirs V. Choosing the right cell line for breast cancer research. *Breast Cancer Res*. 2011;13(4):215.

50. Livasy CA, Karaca G, Nanda R, et al. Phenotypic evaluation of the basal-like subtype of invasive breast carcinoma. *Mod Pathol*. 2006;19(2):264–271.

51. Maheswaran S, Sequist LV, Nagrath S, et al. Detection of mutations in EGFR in circulating lung-cancer cells. *N Engl J Med*. 2008;359(4):366–377.

52. Yu M, Bardia A, Wittner BS, et al. Circulating breast tumor cells exhibit dynamic changes in epithelial and mesenchymal composition. *Science*. 2013;339(6119):580–584.

53. Lecharpentier A, Vielh P, Perez-Moreno P, Planchard D, Soria J, Farace F. Detection of circulating tumour cells with a hybrid (epithelial/mesenchymal) phenotype in patients with metastatic non-small cell lung cancer. *Br J Cancer*. 2011;105(9):1338–1341.

54. Yang J, Weinberg RA. Epithelial-mesenchymal transition: at the crossroads of development and tumor metastasis. *Dev Cell*. 2008;14(6):818–829.

55. Ali S, Coombes RC. Estrogen receptor alpha in human breast cancer: occurrence and significance. *J Mammary Gland Biol Neoplasia*. 2000;5(3):271–281.

56. Thiery JP, Lim CT. Tumor dissemination: an EMT affair. *Cancer Cell*. 2013;23(3):272–273.

57. Yang J, Huang Y, Wang X, Wang X-B, Becker FF, Gascoyne PR. Dielectric properties of human leukocyte subpopulations determined by electrorotation as a cell separation criterion. *Biophys J*. 1999;76(6):3307–3314.

58. Evans E, Yeung A. Apparent viscosity and cortical tension of blood granulocytes determined by micropipette aspiration. *Biophys J*. 1989;56(1):151.

59. Kawata M, Koinuma D, Ogami T, et al. TGF-β-induced epithelial-mesenchymal transition of A549 lung adenocarcinoma cells is enhanced by pro-inflammatory cytokines derived from RAW 264.7 macrophage cells. *J Biochem*. 2012;151(2):205–216.

60. Liu X. Inflammatory cytokines augments TGF-β1-induced epithelial–mesenchymal transition in A549 cells by up-regulating TβR-I. *Cell Motil Cytoskeleton*. 2008;65(12):935–944.

61. Sun JJ, Zhou XD, Liu YK, et al. Invasion and metastasis of liver cancer: expression of intercellular adhesion molecule 1. *J Cancer Res Clin Oncol*. 1999;125(1):28–34.

62. Sununliganon L, Singhatanadgit W. Highly osteogenic PDL stem cell clones specifically express elevated levels of ICAM1, ITGB1 and TERT. *Cytotechnology*. 2012;64(1):53–63.

63. Strakova Z, Livak M, Krezalek M, Ihnatovych I. Multipotent properties of myofibroblast cells derived from human placenta. *Cell Tissue Res*. 2008;332(3):479–488.

64. Lustberg MB, Balasubramanian P, Miller B, et al. Heterogeneous atypical cell populations are present in blood of metastatic breast cancer patients. *Breast Cancer Res*. 2014;16(2):R23.

65. Joosse SA, Pantel K. Biologic challenges in the detection of circulating tumor cells. *Cancer Res*. 2013;73(1):8–11.